Chinese Chemical Letters 37 (2026) 112110

Contents lists available at ScienceDirect

Chinese Chemical Letters

journal homepage: www.elsevier.com/locate/cclet

Highly efficient and ultralong organic phosphorescence by doping crown ether derivatives into polymer

Kejia Ling[a,1], Shunjie Li[a,1], Yuefei Wang[a], Huanyu Yang[a], Zhicheng Song[b], Xian Li[a], Suzhi Cai[a,*], Xiao Wang[c,*], Zhongfu An[b,*]

[a] Strait Institute of Flexible Electronics (SIFE, Future Technologies), Fujian Key Laboratory of Flexible Electronics, Fujian Normal University and Strait Laboratory of Flexible Electronics (SLoFE), Fuzhou 350117, China
[b] State Key Laboratory of Flexible Electronics (LoFE) & Institute of Advanced Materials (IAM), School of Flexible Electronics (Future Technologies), Nanjing Tech University (NanjingTech), Nanjing 211816, China
[c] Institute of Flexible Electronics (IFE, Future Technologies), Xiang'an Campus, Xiamen University, Xiamen 361102, China

ARTICLE INFO

Article history:
Received 24 June 2025
Revised 9 November 2025
Accepted 11 November 2025
Available online 13 November 2025

Keywords:
Ultralong organic phosphorescence
Crown ether
Host-guest system
Hydrogen bonding
Afterglow decorations

ABSTRACT

Ultralong organic phosphorescence (UOP) materials have attracted increasing attention due to its potential applications in opto-electronics, bioelectronics, and security protection. However, it is still a formidable challenge to develop a material with simultaneous efficiency and lifetime enhancement under ambient conditions. Here, highly efficient UOP is achieved by doping crown ether derivatives into rigid poly(vinyl alcohol) (PVA) matrix. Two crown ether derivatives exhibited weak yellow UOP. Impressively, after doped into PVA films, the resultant PVA films demonstrated bright blue UOP with a long lifetime of 595.9 ms and high phosphorescence efficiency of 13.3 %. The sharp enhancement of efficiency and lifetime can be ascribed to abundant hydrogen bonding between the crown ether derivatives and PVA polymer chains. This work provides a new avenue for developing highly efficient UOP materials.

© 2026 Published by Elsevier B.V. on behalf of Chinese Chemical Society and Institute of Materia Medica, Chinese Academy of Medical Sciences.

Ultralong organic phosphorescence (UOP) materials have attracted considerable attention, owing to their low cost, excellent processability, and superior biocompatibility compared with inorganic and metal-organic materials [1,2]. These materials showed potential applications in optical sensing [3–5], bioimaging [6,7], and information encryption [8–10]. However, achieving high-performance UOP remains a great challenge due to weak spin-orbit coupling (SOC) and intense non-radiative relaxation of triplet excitons [11,12]. Therefore, there are two key approaches to constructing efficient UOP: (i) Facilitating the intersystem crossing (ISC) from singlet to triplet states by the introduction of heavy atoms (Cl, Br) [13,14], heteroatoms (O, N, S, P) [15,16], or aromatic carbonyl groups [17]; and (ii) reducing non-radiative decay of triplet excitons through H-aggregation [18,19], crystal engineering [20,21], host-guest doping [22–29], and so on [30,31]. Recently, the researchers proposed a series of strategies of simultaneously improving efficiency or lifetime of organic phosphorescence, such as supramolecular self-assembly based on cocrystals [32], copolymerization [33], host-guest interaction [34,35], among others [36–40]. Although impressive results have been accomplished, organic materials with both long phosphorescence lifetimes (τ_P) and high phosphorescence quantum yields (Φ_P) are rare.

Crown ethers, as the first generation of macrocycles in supramolecular chemistry, represent an intriguing molecular scaffold for designing organic phosphorescent systems [41]. The structural tunability of crown ether derivatives enables precise modulation of their photophysical properties through systematic variations in ether chain length and targeted functional group modifications [42–44]. The oxygen atoms within the crown ether framework can not only facilitate the ISC to populate the triplet excitons [45], but also provide host-guest interactions to enhance conformational rigidity [46,47]. Consequently, crown ethers have been employed to construct functional phosphorescence materials. For example, Tang and coworkers discovered a maximum 10-fold increase of phosphorescence lifetime after traditional crown ethers interacted with potassium ion (K^+) [42]. Similarly, Pan group reported phosphorescence property of crown ethers was greatly enhanced upon complexation with $CdCl_2$, owing to heavy atom effect and abundant intermolecular hydrogen bonds [48]. Moreover, Huang group designed and prepared a random copolymer of acrylamide and a crown ether derivative, the copolymer exhibits satisfactory room

* Corresponding authors.
E-mail addresses: ifeszhcai@fjnu.edu.cn (S. Cai), ifexwang@xmu.edu.cn (X. Wang), iamzfan@njtech.edu.cn (Z. An).
[1] These authors contributed equally to this work.

https://doi.org/10.1016/j.cclet.2025.112110
1001-8417/© 2026 Published by Elsevier B.V. on behalf of Chinese Chemical Society and Institute of Materia Medica, Chinese Academy of Medical Sciences.

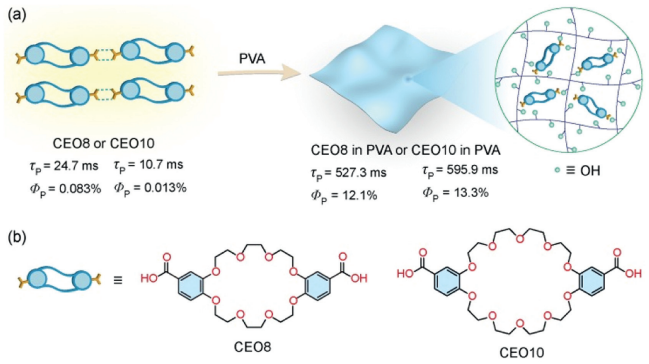


Fig. 1. (a) Schematic diagram of achieving highly efficient and ultralong organic phosphorescence by doping CEO8 and CEO10 into PVA. (b) Chemical structures of CEO8 and CEO10.

temperature phosphorescence [43]. In another study, Wu and colleagues endowed polyacrylamide hydrogels with room temperature phosphorescence through the aggregation-induced crystallization of crown ethers [47]. Despite these advances, UOP polymers containing crown ethers often suffer from phase separation due to the intrinsic poor solubility of crown ether units.

To address the aforementioned issues, we propose a chemical modification strategy to obtain highly efficient UOP homogeneous polymers based on crown ethers (Fig. 1a). Two crown ethers were modified with carboxyl groups to produce two crown ether derivatives, namely, CEO8 and CEO10 (Fig. 1b). Their chemical structures were confirmed by ^{1}H NMR and ^{13}C NMR spectroscopy (Fig. 1b, Figs. S1-S13, Schemes S1 and S2 in Supporting information). Homogeneous polymer films were then fabricated by doping CEO8 or CEO10 into PVA matrix. Compared with the powder counterpart, the phosphorescence lifetime significantly increased from 10.7 ms to 595.9 ms for 2 wt% CEO10 in PVA films. Meanwhile, the phosphorescence quantum yield rose from nearly 0 in the powder state to 13.3 % for 0.5 wt% CEO10 in PVA films. The control experimental results revealed that the phosphorescence originated from isolated crown ether derivative molecules, and hydrogen bonding between crown ether derivatives and PVA polymer chains restrict the molecular vibration and rotation of the guests, thus contributing to highly efficient and ultralong phosphorescence. In addition, these UOP materials have been successfully applied in afterglow decorations.

Both CEO8 and CEO10 powders showed weak blue emission with the peak at 351 nm excited by 272 nm and faint yellow phosphorescence with the emission peak at 543 nm after the removal of the excitation source (Fig. 2a). The phosphorescence lifetime of CEO8 and CEO10 powders are 24.7 ms and 10.7 ms, respectively, corresponding to a short-lived yellow afterglow (Fig. S14 in Supporting information). Transparent PVA films doped with different doping concentrations of CEO8 and CEO10 were prepared *via* a drop-casting method. Interestingly, these transparent PVA films exhibited bright blue emission under 275 nm UV irradiation, which persisted even after the light source was turned off. Yellow UOP from CEO8 and CEO10 in powder and blue UOP from 1 wt% CEO8 in PVA and 1 wt% CEO10 in PVA can be ascribed to the aggregated and isolated phosphorescence chromophores, respectively. As shown in Fig. 2b and Fig. S16 (Supporting information), PVA films showed a polarized photoluminescence emission. Excitation-photoluminescence emission mapping of 1 wt% CEO8 in PVA was collected from the edge of films, exhibiting intense emission peaks at 328 nm (1.3 ns) and 433 nm, while 1 wt% CEO8 in PVA showed intense emission at 328 nm and relatively weak emission at 433 nm when excitation-photoluminescence emission mapping was collected from the front of films (Figs. S15 and S16, Table S1 in Supporting information). The lifetimes of 1 wt% CEO8 in PVA monitoring at 438 nm are 491.6 ms at the edge and 330.5 ms from the front (Fig. 2c, Fig. S17 and Table S2 in Supporting information). Accordingly, photoluminescence and phosphorescence spectra, excitation-phosphorescence emission mapping, and lifetimes are recorded from the edge of films (Figs. S15, S18, and S21-S25 in Supporting information). Phosphorescence emission of 1 wt% CEO8 in PVA and 1 wt% CEO10 in PVA did not change with the excitation wavelength, indicating uniform dispersion of the dopants within the PVA matrix (Fig. S18 in Supporting information). In other words, no phase separation was observed in the PVA films, which was further confirmed by fluorescence microscope images of CEO8-doped PVA films at different concentrations (Figs. S19 and S20 in Supporting information).

To optimize the doping concentration of guests on the UOP properties, PVA films doped with CEO8 and CEO10 at different concentrations were prepared. Their photoluminescence and phosphorescence spectra are similar, but two emission peaks of photoluminescence spectra varied with the doping concentration (Figs. S21 and S22). The phosphorescence intensity of PVA films progressively increased as the doping concentration rose from 0.05 wt% to 2 wt%, but decreased at 3 wt% due to phase separation and aggregation-caused quenching (Fig. 2d). Correspondingly, phosphorescence lifetimes of PVA films followed a similar trend with increasing concentration (Figs. S24 and S25 in Supporting information). Ultimately, the optimal doping concentration of PVA films doped with CEO8 and CEO10 was determined to be 2 wt%. Their longest phosphorescence lifetime of PVA films doped with CEO8 and CEO10 are 527.3 ms and 595.9 ms, respectively (Figs. S24 and S25, Table S2). The blue afterglow can last 6 s after the cease of excitation (Figs. S26 and S27 in Supporting information). The phosphorescence quantum yields of PVA films doped with CEO8 and CEO10 sharply increased compared with those of their corresponding powder (Fig. 2e). The highest phosphorescence efficiency is 12.1 % for 0.1 wt% CEO8 in PVA film and 13.3 % for 0.5 wt% CEO8 in PVA film (Table S3 in Supporting information).

We then measured temperature-dependent photoluminescence spectra and lifetime decay profiles of 1 wt% CEO8 in PVA and 1 wt% CEO10 in PVA over the temperature range of 110–350 K, in order to confirm the phosphorescence property of emission. As expected, the emission intensity of photoluminescence spectra remained nearly constant from 110 K to 170 K, and decreased with the increasing temperature from 170 K to 350 K (Fig. 3a and Fig. S28 in Supporting information), suggesting the emission at 438 nm belong to phosphorescence emission. Consistently, the lifetimes of PVA films doped with crown ether derivatives decreased with varying the temperature from 140 K to 350 K (Figs. 3b and c, Tables S4 and S5 in Supporting information), further confirming the phosphorescence property of emission.

Aiming to investigate the influence of the complexation with K^+, Na^+, and Li^+ ions on phosphorescence properties, 1 wt% CEO8-M^+ (M = Li, Na, K) in PVA films and 1 wt% CEO10-M^+ (M = Li, Na, K) in PVA films were prepared. Photoluminescence and phosphorescence spectra of 1 wt% CEO8-M^+ (M = Li, Na, K) in PVA films and 1 wt% CEO10-M^+ (M = Li, Na, K) in PVA films are similar to those of the corresponding uncomplexed films (Fig. 2a and Fig. S29 in Supporting information). However, their phosphorescence lifetimes are shorter than that of 1 wt% CEO8 in PVA films (491.6 ms) and 1 wt% CEO10 in PVA films (478.3 ms) (Figs. S24, S25, and S30 in Supporting information). After the complexation of crown ether derivatives with metal ions (Li^+, Na^+, and K^+), the phosphorescence lifetime and blue afterglow of the doped PVA films declines gradually with increasing radius of the metal ions (Li^+, Na^+, and K^+) (Figs. S30 and S31 in Supporting information). Phosphorescence quantum yields of the doped PVA films also decreased upon the formation of complexes between CEO8 or CEO10 and Li^+, Na^+, or K^+ (Table S3).

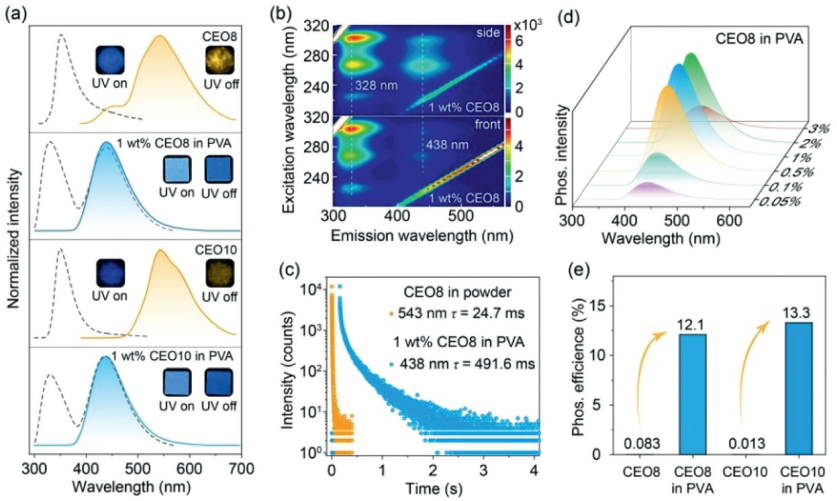


Fig. 2. Photophysical properties of guests in powder and doped into PVA films under ambient conditions. (a) Normalized steady-state photoluminescence (dash lines) and phosphorescence spectra (solid lines) of CEO8 and CEO10 in powder, 1 wt% CEO8 in PVA film, and 1 wt% CEO10 in PVA film. Inset: Photographs of CEO8 and CEO10 in powder excited by 365 nm, 1 wt% CEO8 in PVA film and 1 wt% CEO10 in PVA film excited by 275 nm. (b) Excitation-photoluminescence emission mapping of 1 wt% CEO8 in PVA collected from the edge (top) or the front (bottom). (c) Lifetime decay profiles of CEO8 in powder and 1 wt% CEO8 in PVA films. (d) Phosphorescence spectra of CEO8 in PVA at various concentrations excited by 290 nm. (e) Phosphorescence efficiencies of the guests in powder and the guests doped into PVA films.

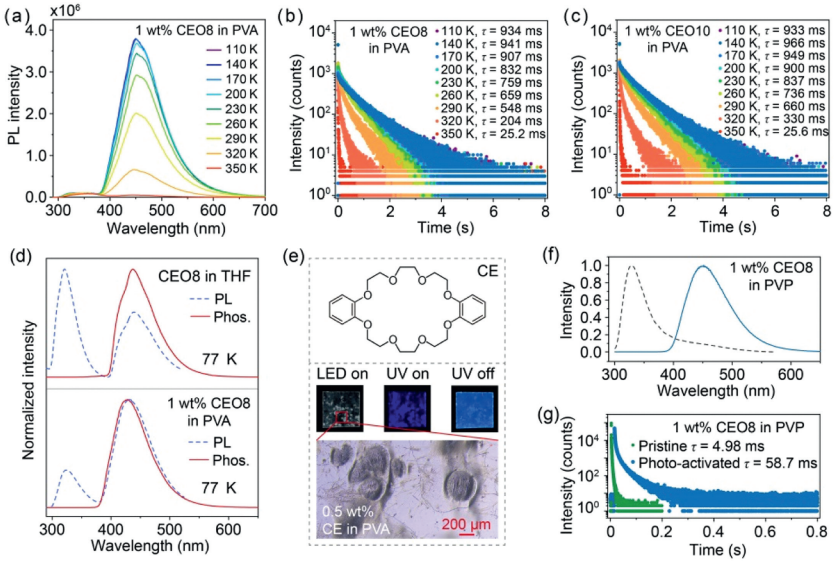


Fig. 3. (a) Temperature-dependent photoluminescence spectra of 1 wt% CEO8 in PVA at different temperatures ranging from 110 K to 350 K. Lifetime decay profiles of (b) 1 wt% CEO8 in PVA and (c) 1 wt% CEO10 in PVA at different temperatures ranging from 110 K to 350 K. (d) Normalized steady-state photoluminescence (dash lines) and phosphorescence spectra (solid lines) of CEO8 in THF (1×10^{-5} mol/L) (top) and 1 wt% CEO8 in PVA (bottom) at 77 K. (e) The chemical structure of CE, luminescent photos and fluorescence microscope image of 0.5 wt% CE in PVA. (f) Normalized steady-state photoluminescence (dash line) and phosphorescence spectra (solid line) of 1 wt% CEO8 in PVP at room temperature. (g) Lifetime decay profiles of 1 wt% CEO8 in PVP at room temperature.

For a deeper insight into the mechanism of UOP, a set of control experiments were conducted. The phosphorescent behaviors of CEO8 and CEO10 in tetrahydrofuran (THF, 1×10^{-5} mol/L) and in PVA films at 77 K were investigated. Notably, the emission profile and peaks of 1 wt% CEO8 in PVA are similar with that of CEO8 in THF (Fig. 3d). Therefore, it can be reasonably inferred that phosphorescence originates from the isolated guest molecules. Natural transition orbitals (NTOs) for theoretically simulated CEO8 and CEO10 in monomer revealed that the phosphorescence chromophores of CEO8 and CEO10 are 3,4-dimethoxybenzoic acid (MOA) group (Figs. S32 and S33 in Supporting information). Theoretically, for isolated CEO8 and CEO10 monomers, there are four main transitions from S_1 to T_n ($S_1 \rightarrow T_7$, T_8, T_9 and T_{10}) for intersystem crossing ($\Delta E_{ST} < 0.3$ eV) (Fig. S34 in Supporting information). The calculated energy levels of a CEO8 and CEO10 monomer at the lowest singlet ($E_{S1} = 4.51$ eV) and triplet excited states ($E_{T7} = 4.58$ eV and $E_{T8} = 4.58$ eV) are considerably close, which enables the facilitation of single-triplet intersystem crossing processes. It was further confirmed by the largest spin-orbital coupling (ξ) constants of CEO8 and CEO10 monomer between S_1 and T_7, T_8 (Fig. S34 in Supporting information).

Considering MOA is the phosphorescence chromophore of CEO8 and CEO10, MOA as a control compound was synthesized (Scheme S3 and Fig. S35 in Supporting information). The photoluminescence (PL) and phosphorescence spectra of MOA in powder form closely resemble those of CEO8 and CEO10 in powder, while the PL and phosphorescence spectra of MOA in PVA match those of CEO8 and CEO10 in PVA (Fig. S36 in Supporting information). It further confirms that the MOA structure serves as the phosphorescent chromophore of CEO8 and CEO10. CEO8 and CEO10 powders

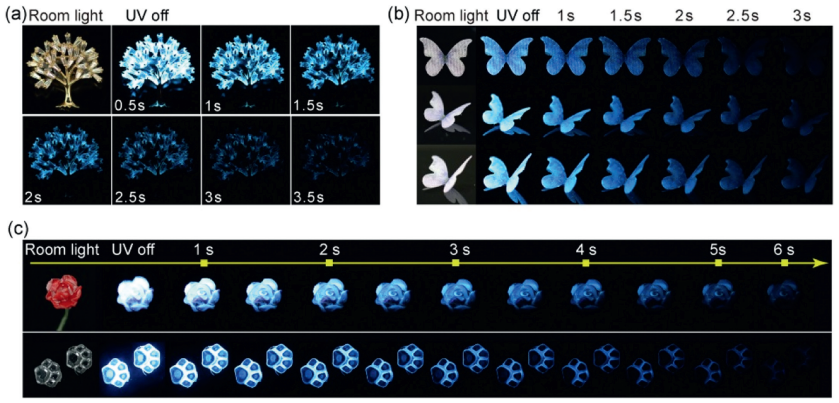


Fig. 4. Photographs of (a) brooch, (b) butterfly, (c) rose and two bear's paw coatings by 1 wt% CEO8 in PVA under room light and a 275-nm lamp off.

showed yellow afterglow with the lifetime of 24.7 ms and 10.8 ms respectively, longer than that of MOA (5.3 ms) (Figs. S14 and S37 in Supporting information). The triplet exciton quenching was significantly suppressed by the crown ether's macrocyclic structure. 1 wt% MOA in PVA, 1 wt% CEO8 in PVA, and 1 wt% CEO10 in PVA films contain the phosphorescence chromophore of 10.98, 7.45, and 6.40 mmol, respectively. Phosphorescence lifetimes of 1 wt% CEO8 in PVA and 1 wt% CEO10 in PVA films are longer than that of 0.5 wt% MOA in PVA, and shorter than that of 1 wt% MOA in PVA (Figs. S24, S25, and S37 in Supporting information). The phosphorescence lifetime highly depended on the concentration of phosphorescence chromophore MOA in PVA.

The role of hydrogen bonding in modulating UOP was further examined using a crown ether (CE) without carboxyl groups as the guest (Fig. 3e). CE-doped PVA films exhibited a short blue afterglow (Fig. 3e and Fig. S38 in Supporting information). We can observe obvious phase separation of 0.5 wt% CE in PVA (Fig. 3e and Fig. S39 in Supporting information), which can be ascribed to the absence of carboxyl groups. These results suggest that carboxyl groups from CEO8 and CEO10 not only promote uniform dispersion of the guest in PVA to avoid the phase separation, but also provide hydrogen bonding sites to restrict molecular motion of the guest, thus prolonging the UOP lifetime.

To demonstrate the formation of hydrogen bonds after doping, Fourier transform infrared spectroscopy (FT-IR) was conducted. The FT-IR of 1 wt% CEO8 in PVA and 1 wt% CEO10 in PVA are similar to that of pristine PVA (Fig. S40 in Supporting information), suggesting that a trace amount of guest molecules does not disrupt the intermolecular interactions and aggregation of PVA polymer. As shown in Fig. S41 in Supporting information, the hydrogen positions a (7.03 ppm) and c (7.53 ppm) on CEO8 and CEO10 exhibited significant chemical shifts after CEO8 and CEO10 were doped into PVA polymer, which can be ascribed to hydrogen bonding between the hydroxyl groups of PVA and the hydrogen atoms at positions a and c on CEO8 and CEO10 molecules. To thoroughly investigate hydrogen bonding, a negative control experiment was conducted. 1 wt% CEO8 in polyvinylpyrrolidone (PVP) showed weak UOP with the lifetime of 4.98 ms (Figs. 3f and g). After photoactivation, phosphorescence spectra can be collected, its phosphorescence lifetime was prolonged up to 58.7 ms (Figs. 3f and g), still markedly shorter than that of the PVA-based system. Because hydrogen bonding between CEO8 and PVP is weaker than that of in PVA. Collectively, phosphorescence of PVA films doped with crown ether derivatives originate from the isolated guest molecules. Hydrogen bonding between the crown ether derivatives and the host matrix plays a crucial role in highly efficient UOP.

Given the feature of excellent UOP property, outstanding processability, and high transparency of PVA, afterglow-coated objects were fabricated. A brooch composed of glass and metal was immersed in an aqueous PVA solution containing 1 wt% CEO8, allowing a uniform coating to form on its surface. After coated with 1 wt% CEO8 in PVA, the appearance of brooch remains unchanged under room light, but showed blue afterglow for several seconds (Fig. 4a). Similarly, a cloth butterfly was fabricated using the same method, its wings could be folded into different postures, and the white butterfly turned blue after turning the UV lamp off (Fig. 4b). In addition, a resin red rose and a glass claw were immersed in the solution and dried, exhibited a striking afterglow (Fig. 4c). These results demonstrate that PVA films doped with CEO8 or CEO10 are highly promising for applications in luminescent coatings and afterglow displays.

In summary, we presented a facile strategy to enhance phosphorescence efficiency and lifetime of crown ether derivatives simultaneously. Two crown ether derivatives, CEO8 and CEO10, were designed and synthesized. While both exhibited weak yellow room-temperature phosphorescence in the solid state, doping into PVA films dramatically prolonged the phosphorescence lifetime from 10.7 ms for powered CEO10 to 595.9 ms for 2 wt% CEO10 in PVA, and phosphorescence efficiency was sharply enhanced from approximate 0 % for CEO10 in power to 13.3 % for 0.5 wt% CEO10 in PVA. A series of control experiments proved the phosphorescence from PVA films originated from the isolated guest molecules. Hydrogen bonding between the crown ether derivatives and the PVA matrix was shown to play a crucial role in achieving highly efficient UOP. Additionally, the carbonyl groups from crown ether derivatives can not only avoid the phase separation, but also restrict the molecular motions of the guests, thus enhancing the UOP emission. Finally, we have successfully applied these PVA film in the field of afterglow artworks. These results provide a strategy to achieve highly efficient UOP and expand the potential applications of UOP materials.

Declaration of competing interest

The authors declare that they have no known competing financial interests or personal relationships that could have appeared to influence the work reported in this paper.

CRediT authorship contribution statement

Kejia Ling: Writing – original draft, Investigation, Data curation. **Shunjie Li:** Formal analysis, Data curation. **Yuefei Wang:** Visualization, Methodology, Formal analysis. **Huanyu Yang:** Methodology, Formal analysis. **Zhicheng Song:** Investigation. **Xian Li:** Investigation. **Suzhi Cai:** Writing – review & editing, Supervision, Project administration, Investigation, Formal analysis, Conceptualization.

Xiao Wang: Writing – review & editing, Resources. **Zhongfu An:** Writing – original draft, Supervision, Resources, Project administration, Investigation, Conceptualization.

Acknowledgments

This work is supported by the National Natural Science Foundation of China (Nos. 52473169, 62288102, 62305276), Fujian Province Natural Science Foundation of China (Nos. 2025J09035, 2024J09014), the Fundamental Research Funds for the Central Universities (No. 1361ZK1007).

Supplementary materials

Supplementary material associated with this article can be found, in the online version, at doi:10.1016/j.cclet.2025.112110.

References

[1] M. Wang, W. Yin, Y. Zhai, et al., Nat. Commun. 16 (2025) 2455.
[2] W. Zhao, Z. He, B. Tang, Nat. Rev. Mater. 5 (2020) 869–885.
[3] X. Li, Y. Wang, Z. Zhang, et al., Adv. Mater. 36 (2024) 2308290.
[4] G. Zhang, G.M. Palmer, M.W. Dewhirst, C.L. Fraser, Nat. Mater. 8 (2009) 747–751.
[5] P. Jiang, B. Ding, J. Yao, et al., Angew. Chem. Int. Ed. 64 (2025) e202421036.
[6] Z. He, H. Gao, S. Zhang, et al., Adv. Mater. 31 (2019) 1807222.
[7] L. Zhang, J. Li, Y. Zhang, et al., Nat. Commun. 16 (2025) 3970.
[8] R. Huang, Y. He, J. Wang, et al., Nat. Commun. 15 (2024) 1596.
[9] H. Deng, G. Li, H. Xie, et al., Angew. Chem. Int. Ed. 63 (2024) e202317631.
[10] G. Lu, J. Tan, H. Wang, et al., Nat. Commun. 15 (2024) 3705.
[11] J. Deng, D. Liu, H. Liu, et al., Adv. Funct. Mater. 34 (2024) 2408821.
[12] S. Xiong, Y. Xiong, D. Wang, et al., Adv. Mater. 35 (2023) e2301874.
[13] T. Zhu, T. Yang, Q. Zhang, W.Z. Yuan, Nat. Commun. 13 (2022) 2658.
[14] L. Ma, S. Sun, B. Ding, X. Ma, H. Tian, Adv. Funct. Mater. 31 (2021) 2010659.
[15] Z. Wang, X. Cheng, Y. Xie, et al., CCS Chem. 5 (2023) 292–309.
[16] K. Zhang, L. Peng, X. Liu, et al., Angew. Chem. Int. Ed. 62 (2023) e202300927.
[17] A.J. Gillett, C. Tonnele, G. Londi, et al., Nat. Commun. 12 (2021) 6640.
[18] E. Lucenti, A. Forni, C. Botta, et al., J. Phys. Chem. Lett. 8 (2017) 1894–1898.
[19] Z. An, C. Zheng, Y. Tao, et al., Nat. Mater. 14 (2015) 685–690.
[20] Z. Chen, X. Chen, D. Ma, et al., J. Am. Chem. Soc. 145 (2023) 16748–16759.
[21] J. Song, L. Ma, S. Sun, H. Tian, X. Ma, Angew. Chem. Int. Ed. 61 (2022) e202206157.
[22] H. Hou, H. Wang, M. He, et al., Angew. Chem. Int. Ed. 63 (2024) e202411323.
[23] C. Chen, W. Zhang, Z. Wang, et al., Angew. Chem. Int. Ed. 64 (2025) e202501448.
[24] L. Wei, S. Guo, B. Zhang, et al., Adv. Funct. Mater. 34 (2024) 2409681.
[25] L. Jin, Z. Wang, W. Mo, et al., Angew. Chem. Int. Ed. 63 (2024) e202410974.
[26] L. Jiang, Z. Qian, Y. Chen, et al., Chin. Chem. Lett. 36 (2025) 110676.
[27] Z. Chen, J. Shi, Y. Zhou, P. Zhang, G. Liang, Chin. Chem. Lett. 36 (2025) 110629.
[28] J. Zhou, D. Liu, L. Li, et al., Chin. Chem. Lett. 35 (2024) 16300–16306.
[29] H. Yao, F. Yang, J. Hu, et al., Chin. Chem. Lett. 36 (2025) 110375.
[30] F. Nie, D. Yan, Nat. Commun. 15 (2024) 9491.
[31] Y. Xu, Z. Cheng, H. Wang, et al., Adv. Opt. Mater. 13 (2024) 2402607.
[32] Z. Chen, Z. Chen, Y. Zhu, et al., Adv. Funct. Mater. 34 (2024) 2408023.
[33] X. Fan, L. Gao, Y. Jin, et al., Adv. Opt. Mater. 13 (2024) 2402627.
[34] P. Chen, H. Qie, X. Yang, et al., Adv. Funct. Mater. 35 (2024) 2416430.
[35] Z. Wu, Z. Xu, D. Wang, et al., Adv. Funct. Mater. 35 (2024) 2415285.
[36] V. Kumar, G. Venugopal, A.B. Jadhav, et al., Angew. Chem. Int. Ed. 64 (2025) e202422125.
[37] A. Huang, Y. Fan, K. Wang, et al., Adv. Mater. 35 (2023) 2209166.
[38] Z. Yang, H. Liu, X. Zhang, et al., Adv. Mater. 36 (2023) 2306784.
[39] J. Wei, C. Chen, M. Xiao, et al., FlexMat 2 (2025) 180.
[40] Y. Lu, X. Chen, Y.D. Suh, et al., FlexMat 2 (2025) 107.
[41] C.J. Pedersen, J. Am. Chem. Soc. 89 (1967) 7017–7036.
[42] P. Wei, X. Zhang, J. Liu, et al., Angew. Chem. Int. Ed. 59 (2020) 9293–9298.
[43] W. Zhu, H. Xing, E. Li, H. Zhu, F. Huang, Macromolecules 55 (2022) 9802–9809.
[44] W. Zhu, B. Zhao, S. Fang, H. Zhu, F. Huang, Chem. Sci. 15 (2024) 16300–16306.
[45] Q. Zhou, T. Yang, Z. Zhong, et al., Chem. Sci. 11 (2020) 2926–2933.
[46] H. Wang, W. Xing, Z. Yu, et al., Adv. Opt. Mater. 10 (2022) 2201903.
[47] H. Ju, H. Zhang, L. Hou, et al., J. Am. Chem. Soc. 145 (2023) 3763–3773.
[48] Z. Wang, X. Zhang, J. Mo, C. Su, M. Pan, Adv. Opt. Mater. 11 (2023) 2203144.